

## EXPERIMENTAL INVESTIGATION OF A REAL-LIFE MICROSCALE TRIGENERATION SYSTEM USING ADSORPTION COOLING, REVERSIBLE HEAT-PUMP AND A COGENERATION UNIT

Parantapa A. Sawant<sup>1</sup>, and Jens Pfafferott<sup>1\*</sup>

<sup>1</sup>Institute of Energy System Technologies (INES)  
Offenburg University of Applied Sciences  
Am Güterbahnhof 1a, 77654, Offenburg, Germany  
e-mail: [parantapa.sawant@hs-offenburg.de](mailto:parantapa.sawant@hs-offenburg.de), web page: <http://www.ines.hs-offenburg.de/institut/>

\*Offenburg University of Applied Sciences

**Keywords:** Microscale Trigeneration, Energy Conversion and Management

**Abstract.** *Microscale trigeneration systems are highly flexible in their operation and thus offer the technical possibility for peak load shifting in building demand side management. However to harness their potential modern control methods such as model predictive control must be implemented for their optimal scheduling. In literature the need for experimental investigation of microscale trigeneration systems to identify typical characteristics of the components and their interactions has been identified. On a real-life set-up control specific information of the components is collected and lessons learnt during commissioning of the equipment is shared. The data is analysed to draw the vital characteristics of the system and it will be used for creating models of the components that can be utilised for optimal control.*

### 1 INTRODUCTION

In the European Union buildings account for 40% of the total primary energy consumption and 35 % of the CO<sub>2</sub> emissions<sup>[1]</sup>. For achieving a good building performance which is expressed as the congruous interaction of the building architecture, energy systems and indoor comfort; advanced measuring and control technology combined with a building automation and control system are needed. Here, microscale trigeneration or combined cooling heating and power systems based on adsorption cooling can play a very important role due to their flexibility, high primary energy savings ratio and ability to work with low-temperature waste heat<sup>[2-4]</sup>. To harness their potential of integrating the electricity and gas grid, optimal control technologies have to be employed to schedule these systems predictively instead of the conventional control strategies<sup>[5-7]</sup>. How can an experimental investigation help in achieving this optimal control?

Experimental investigation of a real-life microscale trigeneration lab focusing on identifying important operational characteristics of the components such as their internal safety loops or temperature profiles and their interoperability from a control point-of-view will give an insight into the important features that must be included in the optimal control problem. Existing laboratories have helped either to describe the operation of the individual components or identifying important parameters for their detailed modelling<sup>[8-11]</sup>. Additionally the existing optimal scheduling problems often consider only power flows and energy balances without taking into account the part-load behaviour of the components due to the variations in the line-temperatures or internal control logic of the components. However it has been highlighted that to run the system on the field level the dynamics of the components have to be taken into account<sup>[12]</sup>.

In this paper we describe the advanced microscale trigeneration system that is established at the Institute of Energy System Technologies (INES) in Offenburg, Germany using an adsorption chiller, a reversible heat pump and a combustion based co-generation unit. This complex system was set-up using market ready components for reducing initial investment costs and facilitates a fully grid-reactive operation<sup>[13,14]</sup>.

The important operational and control data of the main and auxiliary components in the system were analysed from the manufacturer's manuals and are presented here along with the instrumentation and data acquisition set-up in the lab. The lessons learnt during installing and commissioning this complex energy network are mentioned. Finally experimental results of the main tests with the components and their outputs are presented.

## 2 EXPERIMENTAL SET-UP OVERVIEW

The experimental set-up at INES is shown in fig. 1 below. The main components with the complex hydraulics can be seen here. The basic and detail engineering, installation of the hardware and programming of the data acquisition and control system has been done in-house.



Figure 1. Microscale trigeneration lab at INES. From left to right: wall mounted Electric Switch Board (ESB), green coloured Combined Heating and Power (CHP), Electric Heating Coil (COIL), Hot Thermal Energy Storage (HTES), Adsorption Chilling Machine (AdCM), Reversible Heat Pump (RevHP), Cold Thermal Energy Storage (CTES)

As seen in the process flow diagram of the plant in fig. 2 the CHP unit converts energy from the fuel into electricity and heat. It is assumed for this project that this electricity is firstly used to cover the energy demands of the entire plant and the electric load from the institute, feeding the remainder into the grid. The waste heat is then stored in a stratified HTES tank. The COIL can convert electricity to heat during peak load hours and also store it in the HTES tank. The heat can be distributed further to cover the thermal load or can be converted into cool (representing cooling energy) using the AdCM. The cool is stored in a CTES tank. In addition to the CHP and AdCM combination a conventional RevHP is integrated into the system. This can produce heat (cool) for storing in the HTES (CTES). The Outdoor Coil (OC) is located outside the institute's main building (not seen in the figure) in the open and acts as the heat sink for the AdCM and CCM and the heat source for the HP. A detailed process and instrumentation diagram and different modes of operation possible with this set-up can be obtained from Sawant *et al.*<sup>[15]</sup>. The details of each component will follow in the next section.

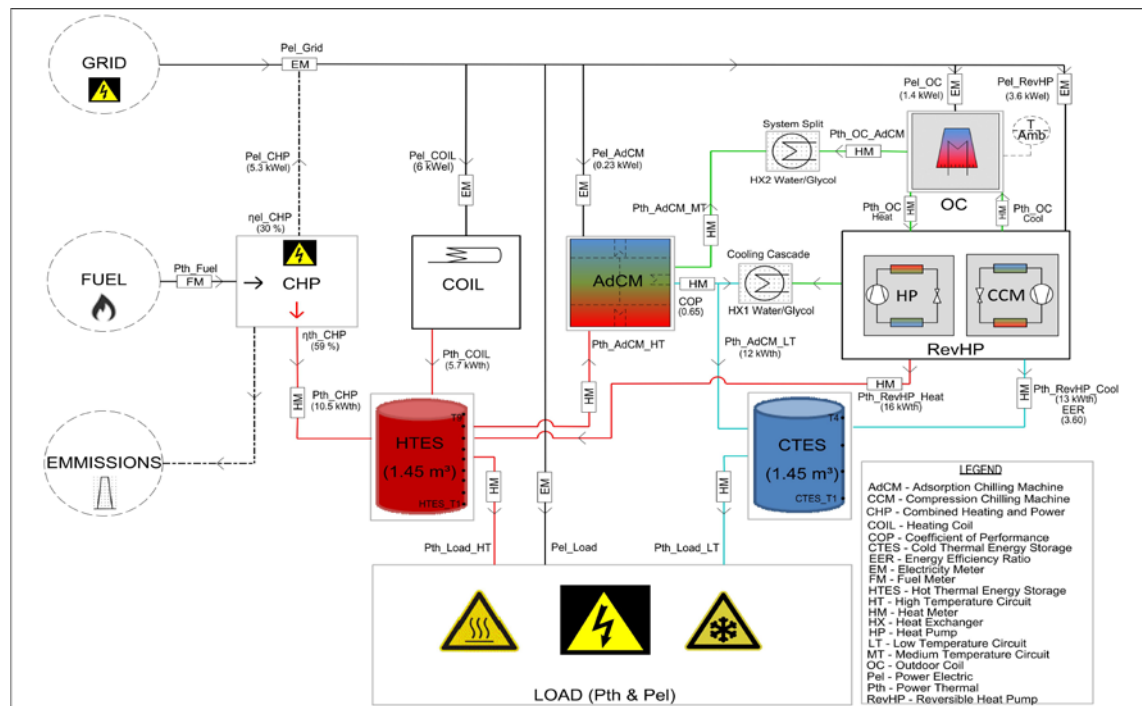


Figure 2. Process flow diagram with instrumentation

### 3 MAIN COMPONENTS

The main components are market-ready machines used typically in microscale trigeneration plants.

#### 3.1 Combined Heat and Power Unit (CHP)

The CHP is a completely overhauled second-hand unit of the type “Dachs HKA HR5.3” manufactured by SenerTec GmbH. The engine is single cylinder, 4-Stroke with approx. 580 cm<sup>3</sup> and can run on fuel oil or bio-diesel. The generator is asynchronous, water cooled and is connected to the engine with a single step gear box. The CHP unit is rated at a thermal power output of 10.5 kW<sub>th</sub> (P<sub>th\_CHP</sub>) and electrical power output of 5.3 kW<sub>el</sub> (P<sub>el\_CHP</sub>) with an auxiliary power consumption of 0.14 kW<sub>el</sub> (+/-10%). The generator works with three phase, 230/400 V and 50 Hz.

The integrated controller (MSR-1) maintains a constant hot water temperature exiting the CHP by varying the volume flow of the cooling water by regulating the cooling pump. The MSR-1 has a safety switch-off when the return line temperature measured internally on the generator inlet exceeds 73 °C. The MSR-1 controller has an initialisation time of 45 seconds when the main switch is turned on and another 45 seconds are needed after that for preparing to start the CHP. However, if the MSR-1 controller was not turned off over the main switch and only the external start signal is given the start-up process then takes only 25 seconds. Thus, if the CHP is started from a supervisory controller, these 25 seconds of start-up must be accounted for assuming the MSR-1 controller is not completely shut-down by the supervisory controller. Additionally for every start the CHP has a minimum run-time of 30-72 mins which is needed to reach exhaust gas temperatures in excess of 100°C for complete combustion of exhaust ashes.<sup>[16]</sup>

The fuel used in the experiments is Aral Heating Oil-EcoPlus having a standard higher heating value of 45.6 MJ/kg and density of 853.5 kg/m<sup>3</sup><sup>[17]</sup>.

#### 3.2 Adsorption Chilling Machine (AdCM)

The adsorption chilling machine (AdCM) is of type “eCoo10” manufactured by SorTech AG. The machine is a two chamber aggregate with each chamber having one Evaporator / Condenser and one Adsorber / Desorber combination. The adsorption / desorption and heat recovery phases are controlled using a complex piping network comprising of 3-way-valves and in-built pumps.

It has a rated maximum cooling capacity (P<sub>th\_AdCM\_LT</sub>) of 12 kW<sub>th</sub> with a maximum co-efficient of performance (COP) of 0.65. The AdCM can work with hot water temperatures (HT Circuit) ranging between 55 °C – 95 °C. The chilled water output temperature (LT Circuit) ranges between 08 °C – 21 °C which can be set using an external 0.5 V – 3.05 V signal. The recommended temperature going to the OC in the re-cooling circuit (MT circuit) is between 22 °C – 40 °C. The nominal volume flow rates in HT, MT and LT circuit are 1.6 m<sup>3</sup>/h, 4.1 m<sup>3</sup>/h and 2 m<sup>3</sup>/h respectively. The recommended volume flow in the MT circuit after the system split going to the OC is 4.8 m<sup>3</sup>/h<sup>[18]</sup>.

The OC rotational speed and the pumps in all the circuits including the one in the system split are controlled optimally by the internal controller of the AdCM. The simplified sense of this controller is to ensure that the temperature in the MT circuit entering the AdCM is always higher than the temperature in the LT circuit entering the machine.

The free cooling, free heating, power mode and heat pump mode of the AdCM are not considered in the scope of this work. Details of these modes can be found in manufacturer data sheets<sup>[18]</sup>.

The auxiliary components necessary are explained in section 4.

#### 3.3 Reversible Heat Pump (RevHP)

An air-water-electricity reversible heat pump (RevHP) using R407C of the type “EWWP/014/KBW/1N” from Daikin is used both as a compression chilling machine (CCM) and as a heat pump (HP). The machine has a nominal cooling (P<sub>th\_CCM</sub>) and heating (P<sub>th\_HP</sub>) capacity of 12.9 kW<sub>th</sub> and 16.7 kW<sub>th</sub> respectively. Its electrical power consumption (P<sub>el\_RevHP</sub>) is specified at 3.8 kW<sub>el</sub> for both heating and cooling. The COP is given as 4.45 and the energy efficiency ratio (EER) is given as 3.44<sup>[19]</sup>.

The nominal volume flows in the evaporator and condenser circuits are 2.22 m<sup>3</sup>/h and 2.88 m<sup>3</sup>/h. In this set-up these volume flows are maintained by external pumps and are not controlled under the scope of this work. These are kept constant for simplicity of control and to maintain the values closest possible to recommended nominal flows.

The operation range is defined between – 10°C and 20 °C for evaporator and 20 °C and 55 °C for condenser. However due to constructional restrictions in the lab at INES we are restricted to a minimum of 5°C in the evaporator circuit. Hence the operation of the HP is possible only with an ambient temperature higher than 12 °C. To ensure a complete range of operation both the circuits must be planned with glycol-water mixture and system splits must be planned accordingly with water only circuits. The switching between HP and CCM must also be planned in the hydraulic circuits and does not occur in the machine internally.

The internal controller of the RevHP allows for defining a cooling / heating set point and a differential

parameter for hysteresis. This internal hysteresis control prevents frequent switching of the machine and its functioning is explained further in section 6.3

### 3.4 Thermal Storage Tanks (HTES and CTES)

The heat and cool is stored using water as a storage medium. The hot thermal energy storage (HTES) tank and the cold thermal energy storage (CTES) tank are 1500 L and 1450 L respectively. The tanks are made of steel of the type St37.1. HTES has 160 mm plastic foam insulation and CTES has 19mm Armaflex diffusion tight<sup>[20]</sup>.

The HTES (CTES) tank is a vertical stratified tank with 9 (4) temperature sensors located inside copper tubes running along the depth of the tank. Here T<sub>1</sub> is at the bottom and T<sub>9</sub> for HTES and T<sub>4</sub> for CTES at the top.

The flow of water in the given HTES is such that hot water from the sources (CHP or HP) enters at the top of the tank and cold water from bottom is returned to them. Hot water for the thermal load is taken from the middle of the tank and cold coming back from the load enters at the bottom of the tank. Furthermore, due to a construction restriction hot water for driving the AdCM is not taken from the top of the tank but from three-fourth of the height of the tank. However, it is highly recommended to use tank constructions in which the AdCM gets the hottest water from the top of the tank. The flow of water in the CTES is relatively simple with the chilled water from the sources (AdCM or CCM) entering at the bottom of the tank and warm water from top is returned back to them. Chilled water for the thermal load is taken from the bottom of the tank (HTES<sub>4</sub>) and warm water coming back from the load enters at the bottom of the tank.

For optimal control where temperature profiles in the tank play an important role for the performance of the connected machine it is important to specify the levels from the tank where the water enters or is withdrawn from. This is unfortunately not the case in most of the works found in literature where for simplicity only the top and bottom layers of the tank are considered for entry or exit of the water flows<sup>[21-23]</sup>.

The CHP hot feed-line enters at the top of the HTES through an internal pipe bending upwards. This construction is most often used for microscale CHP systems since the volume flow of water is low and the temperature difference very high. However the hot water from the HP has a higher volume flow and lower temperature difference and thus another construction is used for feeding it into the tank. Here a stratification tube is built in such a way that the initial flow of cold water after a cold-start of the RevHP unit is collected in a bucket like structure and as hot water begins to flow from the RevHP it rises from this bucket structure to top of the tank through small pipes of diameter 5mm and 10 mm. Details of this construction can be found in the manufacturer's datasheet<sup>[20]</sup>.

### 3.5 Outdoor Coil (OC)

The outdoor coil uses two electric fans with a maximum speed of 900 RPM consuming 0.7 kW each at maximum speed. The heat exchanger area is 221.4 m<sup>2</sup> and thermal power (P<sub>th\_OC</sub>) of 22 kW<sub>th</sub> at design point. The overall heat transfer coefficient is assumed to be 37.49 W/m<sup>2</sup>K.

For simplicity and saving of construction costs the same OC is used for supporting the operation of both the AdCM and the RevHP. During AdCM operation the OC is controlled by the internal controller of the AdCM. For HP the OC is running at maximum speed with a 10 V signal. For CCM the OC is controlled using a rule-based control developed in-house in the LabVIEW® environment.

### 3.6 Electric Heating Coil (COIL)

The hot storage tank is equipped with an immersed electric heating coil that can act as an additional heater for meeting peak loads. The electric heater also gives an opportunity to integrate a power-to-heat mode. The electrical coil is 6 kW<sub>el</sub> and has a thermostat temperature regulator from 5 °C to 85 °C that acts as a safety switch-off<sup>[24]</sup>. The coil produces a surface load between 9.1 – 11.2 W/cm<sup>2</sup>. The coil is located in the HTES at a height corresponding to HTES<sub>3</sub>. For more accurate modelling and control of these systems it is important to include the location of the COIL in the HTES. This point is explained with data under section 6.2.

## 4 AUXILIARY COMPONENTS

The hydraulic components supporting the functioning of the plant are defined here as auxiliary components and will play an important part in the control of the system. Thus they must be accounted for in a supervisory control system that is based on model predictive control.

### 4.1 Heat Exchangers

The system is separated between 34 % glycol-water circuits with a density of 1039.73 kg/m<sup>3</sup> and water-only circuits using two counter-flow plate heat exchangers.

The heat exchanger for AdCM-OC system split is 7.83 m<sup>2</sup>, with an overall heat transfer coefficient of 2172 W/m<sup>2</sup>K. To simplify the set-up this heat-exchanger in the AdCM-OC circuit is also used in the HP\_LT-OC

circuit.

Another heat exchanger splits the system in the HP\_MT – HTES circuit. This is 0.52 m<sup>2</sup> with an overall heat transfer coefficient of 2200 W/m<sup>2</sup>K.

#### 4.2 Three-Way Mixing Valves

For achieving a set-point temperature a 3-way mixing valve is built in the circuit controlled using three-position control. Since the valve actuator doesn't provide a feedback on its position a conventional PID controller couldn't be implemented. Instead a rule-based controller is developed in-house using LabVIEW® which reacts when the error in the controlled variable is greater than 0.5 K. The controller makes changes to the valve position in control steps directly proportional to the size of the error, thereby mixing the return line of the load or taking more water from the tanks. The control step is defined in seconds for which the motor should rotate in the necessary direction. A time delay of 120 s is planned before the next measurement is made and control action is taken since considering the time taken for a change in the value of the temperature sensor. The value of the time delay, error tolerance and step-size is based on values gathered during experiments.

#### 4.3 Heating or Cooling Switch-Over Valves

To switch the hydraulic circuits from heating to cooling of the thermal loads switch-over valves are implemented in the system. The experiments are restricted to either supplying heating or cooling to the thermal load. The actuation time of the switch-over valves is 180 s.

#### 4.4 Ball Valve Actuators

For complete automation of the plant and switching between different modes of operation ball valve-position actuators are installed wherever necessary. The actuation time of these motors is 130 s. In the development of the supervisory controller this time should be accounted for while switching between operational modes.

## 5 INSTRUMENTATION AND DATA ACQUISITION

For the analysis of the entire system operating under different scenarios and to collect data relevant for parameter and state estimation extensive instrumentation has been applied. The temperature of water and water-glycol mixture in all the circuits and in the storages, their volume flow rates, thermal and electrical powers of the components, fuel consumption and ambient temperature are measured. The following table shows the test instrumentation and their accuracies.

Measured Parameter	Instrument	Accuracy
Water Temperature in Storages	PT-1000 Class B (2-lead circuit)	At 0°C ± 0.3 K, at 100°C ± 0.8 K
Water Temperature in Circuits	PT-500 Class B (coupled)	± (0.30 + 0.0050 ·  T ),
Water/Glycol Mixture Temperature	PT-100 Class B (2-lead circuit)	± (0.30 + 0.0050 ·  T ),
Ambient Temperature	PT-100 (2-lead circuit)	(± 0.1 K)
Water Volume Flow	Ultrasonic flow meter	± (2 + 0.02 v <sub>max</sub> /v <sub>real</sub> )
Water/Glycol Mixture Volume Flow	Multi-jet turbine meters with dry- type registers	± (3 + 0.05 v <sub>max</sub> /v <sub>real</sub> )
Fuel Volume Flow	Mechanical roller counter	± 1% · v <sub>real</sub> of actual value
Electricity Power	Electrical power meter	Class 1 and 2 of IEC 1036

Table 1. Instrumentation applied in the microscale trigeneration lab

The ambient temperature sensor (T<sub>amb</sub>) is located at the Outdoor Coil (OC) giving the advantage of measuring the temperature in the vicinity of the OC which is the component interfacing with the environment. Since the temperature sensor is PT100 with a 2-lead circuit, a resistance compensation for the measurement was made. A resistance of 1 Ohm was measured in the approx. 15 m wire from the sensor to the ESB. This resistance is equivalent to 2.0 K for a PT-100 sensor<sup>[25]</sup> and was thus deducted from the measurement of the sensor.

The Data Acquisition and Supervisory Control (DSC) is based on an OPC Client/Server network. The OPC Client is a Beckhoff CX9020® Programmable Logic Controller (PLC) communicating with the physical components and instruments using MBUS standards at a Baudrate of 2400 ms. The OPC server is the Shared Variable Engine in NI-LabVIEW® 2015. The data is logged with change-of-value and the logging dead-band is 2 % of previous value. The logging resolution of temperature, volume flow and power is 0.1 °C, 0.00 m<sup>3</sup>/h and 0.1 kW respectively. The logged data is exported from the LabVIEW® environment with a 60 seconds time interval and a natural interpolation.

## 6 EXPERIMENTAL INVESTIGATION

In the following subsections the main results achieved during the experiments carried out in both winter mode and summer mode will be analysed. The behaviour of the components and their internal control logics are highlighted wherever they could be used in developing the optimal control problem.

### 6.1 Co-generation Unit (CHP) Performance

A number of tests were performed for collecting information on the operational parameters of the CHP unit and its behaviour in combination with the HTES. Here, different initial temperatures in the hot tank were chosen and one of these tests is shown in fig. 3 (a & b) below. At time  $t = 0$  mins the CHP is switched on from a cold state (step function), the initial temperature of the HTES is 20 °C and no loads are connected to the tank. A typical behaviour of a 1<sup>st</sup> order heating system with delay element is noticed. There is a rapid increase in the feed-line temperature of the CHP ( $T_{\text{CHP\_FL}}$ ) from 20 °C to 64 °C in the first 15 mins and the electrical power produced by the CHP ( $P_{\text{el\_CHP}}$ ) increases to almost its nominal value of 5.3 kW<sub>el</sub> in 8 mins of start. For achieving high accuracy the simulation models of such systems must cover this highly dynamic behaviour at the start and then cover the steady state condition. However this makes the models more complex and for application in optimal control often steady state modelling of the CHP is done in the literature <sup>[5,26]</sup>. In this test the steady state is achieved after almost 60 mins where the volume flow ( $v_{\text{dot\_CHP}}$ ), the  $T_{\text{CHP\_FL}}$  and the thermal power produced by the CHP ( $P_{\text{th\_CHP}}$ ) become almost constant. This is in accordance with the internal control of the CHP as mentioned in section 3.1 wherein the volume flow is internally controlled to achieve maximum possible feed-line temperature. Also in accordance to the energy balance in the CHP circuit for a given thermal power, as the return line temperature ( $T_{\text{CHP\_RL}}$ ) increases the volume flow and correspondingly the  $T_{\text{CHP\_FL}}$  increase. This behaviour is exploited to develop analytical models of the CHP unit in some research works by calculating the volume flow as a function of  $T_{\text{CHP\_RL}}$  <sup>[27]</sup>. Since  $v_{\text{dot\_CHP}}$  is also dependent on the hydraulics of the circuit this approach has an added advantage as the  $v_{\text{dot\_CHP}}$  is calculated from experimental data that already considers the hydraulics.

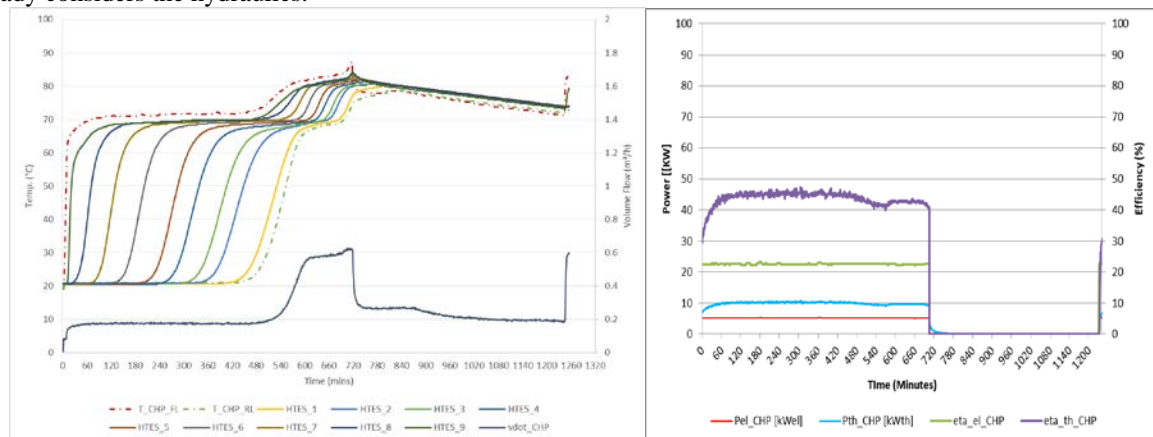


Figure 3 (a & b). Charging of HTES with CHP.

Additionally as seen in the fig. 3a for the steady-state  $P_{\text{th\_CHP}}$  and  $v_{\text{dot\_CHP}}$  only a constant temperature difference is achieved between the feed-line and return-line temperatures thus the stratifications in the HTES occur in two stages with the second stage occurring while the  $T_{\text{RL\_CHP}}$  begins to increase. These stratifications can be seen with the help of the 9 temperature sensors in the HTES. In steady-state there is only a temperature difference of approx. 2 K in the feed-line and return-line the CHP and the corresponding temperature sensors in the HTES. A possible reason for this could be the inaccuracies in the measuring instruments and complex thermal flows occurring within the tank. Since the temperature difference is not so

significant a further analysis is not under the scope of this work.

After around 11.95 hours as the  $T_{CHP\_RL}$  reaches  $73\text{ }^{\circ}\text{C}$  and the CHP automatically shuts-down due to its internal safety control as mentioned in section 3.1. However, a minimum  $\dot{v}_{CHP}$  of  $0.2\text{ m}^3/\text{h}$  is observed in the circuit creating a negative effect of mixing the stratifications and also mixing the  $T_{CHP\_FL}$  and  $T_{CHP\_RL}$ . While applying optimal control these points should be considered as physical constraints so as to avoid the safety-shut down of the CHP and turning the MSR-1 off with supervisory controller so no unnecessary volume flow occurs. Additionally as seen in fig. 3b the  $Pe_{CHP}$  is almost constant at  $5.2\text{ kWel}$  throughout the entire test. However, the  $P_{th\_CHP}$  after entering steady-state is almost constant at  $10.2\text{ kWth}$  and with increasing  $T_{CHP\_RL}$  enters part load behaviour. In part load the  $P_{th\_CHP}$  reduces to  $9.8\text{ kWth}$  before finally it reduces to 0 as the machine shuts down.

## 6.2 Heating Coil (COIL) Performance

The step-response of the temperatures in the HTES to the step function of the COIL is seen in fig.4. The initial temperature in HTES is approx.  $36\text{ }^{\circ}\text{C}$  and after 8 mins the COIL is turned ON. Immediately it begins to consume  $5.9\text{ kWel}$  ( $Pe_{COIL}$ ) in accordance to  $6\text{ kWel}$  rating of the manufacturer considering the inaccuracy of the electricity meter. The temperature in the tank also begins to rise with a time delay of 3 mins.

This time delay arises because the coil is located at the level of HTES\_3 and as it heats the water in this layer, the hot water begins to rise through the tank heating all layers above HTES\_3 with it. This behaviour leads to almost linear heating up of the layers as in a mixed storage tank and must be handled as such in the simulation models of the HTES. However the layers below HTES\_3 i.e the bottom (1<sup>st</sup>) and 2<sup>nd</sup> layer behave differently, with the bottom layer showing almost no increase in temperature. Again as seen in the fig. 4 after 620 mins of operation the COIL shuts-off automatically as HTES\_3 crosses the safety temperature of  $74\text{ }^{\circ}\text{C}$ . Beyond this temperature the COIL frequently switches without any significant rise in the tank temperature.

Thus it is important to mention the location of the COIL in the tank for including the safety shut-off feature at the temperature of the layer where coil is located and layers below the coil-layer do not get influenced by its energy. Only with the exact layer temperature defined the supervisory controller can restrict the COILs operation outside this region.

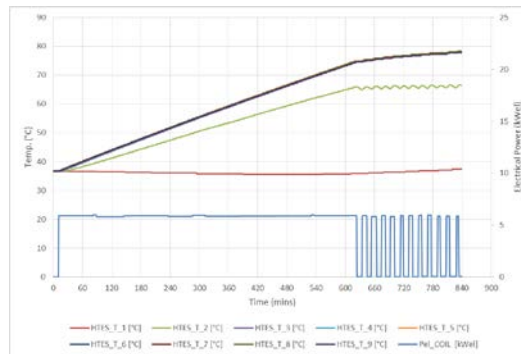


Figure 4. Charging of HTES with COIL

## 6.3 Adsorption Chilling Machine (AdCM) Performance

The temperature fluctuations occurring in the three circuits of the AdCM during two complete cycles due to the internal switching of valves and circuits are shown in fig. 5. Detailed description of this behaviour can be found in the works of Kong *et al.*, Núñez T. and the SorTech Operating Manual<sup>[11,18,28]</sup>. The two chambers are working in tandem and as one is adsorbing the other is desorbing with mass and heat recovery phases occurring between the switching. The inlet temperature going into the machine for the three circuits are almost constant due to the internal control of the machine however the temperatures leaving the machine show large fluctuations. In the HT (LT) circuit fluctuations to almost 10 (8) K are noticed. These fluctuations are reduced to only 2 K due to the dampening effect of the storages as seen in fig.6, with the behaviour of HTES\_1 (CTES\_1) corresponding to the HT (LT) outlet. Thus, simplified analytical models of the AdCM that do not necessarily simulate this fluctuating behaviour could be used in optimal control.

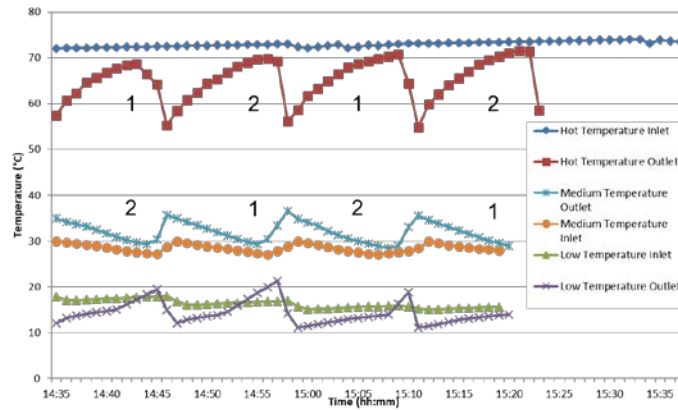


Figure 5. Temperature profiles in the 3 circuits of the AdCM

A test with the AdCM was performed with the HTES and CTES at 80 °C and 20 °C respectively. No other heating / cooling supplies or loads were connected to the tanks. The steady state behaviour is observed in fig. 6 (a & b). The cooling capacity ( $P_{th\_AdCM\_LT}$ ) of the AdCM reduces and the cycle-time increase as the temperatures in the HTES and CTES reduce. This happens because with lower temperatures in the HTES the thermal input to drive the AdCM reduces and with lower temperature in CTES the AdCM works in part-load. This effect in the form of the relationship of the cooling capacity and co-efficient of performance (COP) of the AdCM with the temperatures in the three circuits is quantified in the data sheets of the manufacturer and can be used to develop a simplified model of the machine.

Also it is seen that the HTES temperature reduces in reverse stratification form when the AdCM withdraws hot water from it. Here, the importance to define the layer of the tank from which the AdCM withdraws hot water in the analytical model is realised. The layers above the AdCM feed-line layer remain unaffected. This can be seen in the results that HTES\_8 and HTES\_9 behave differently than the other layers that are directly affected by the AdCM and it is concluded that the ADCM feed-line layer corresponds to HTES\_7. The temperature in the HTES drops from 80 °C to 50 °C after 3 hours of operation. During the same time the CTES cooled down from 22 °C to 10 °C.

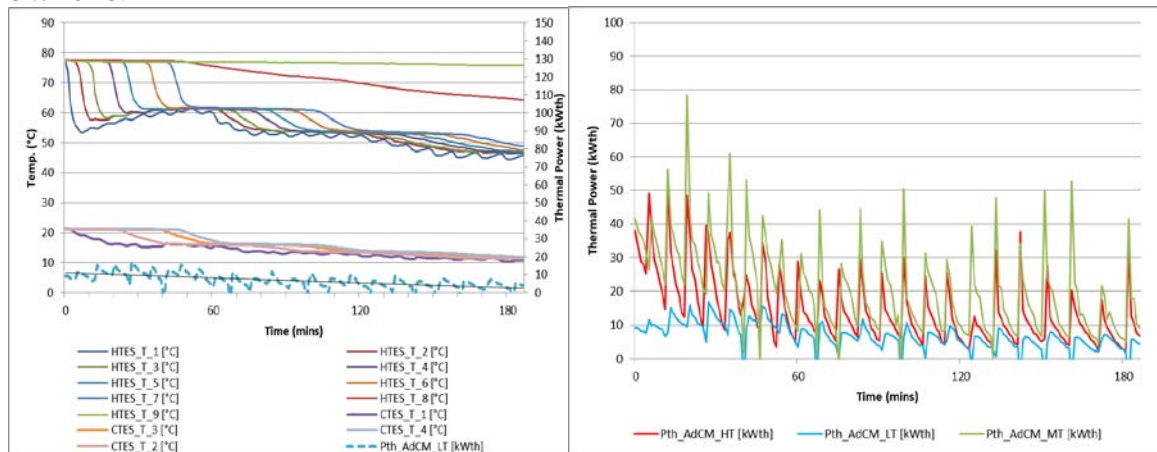


Figure 6 ( a & b). Charging of CTES and Discharging of HTES with AdCM

Another important observation made in fig. 6b is that the approximate sum of the cooling capacity of the AdCM ( $P_{th\_AdCM\_LT}$ ) and its thermal input ( $P_{th\_AdCM\_HT}$ ) is almost equal to the power that is released to the environment in the OC circuit ( $P_{th\_AdCM\_MT}$ ). This behaviour is in accordance to the thermodynamic cycles of the AdCM described in the works of Schickntanz *et al.* and Gräber *et al.* [29,30].

#### 6.4 Reversible Heat Pump (RevHP) as Compression Chilling Machine (CCM) Cooling Performance

Steady state behaviour of the CCM is shown in the results of a test in fig.7 (a & b) below. Here the initial temperature of the CTES is 32 °C and no cooling loads were connected to the tank. The set temperature for the internal hysteresis of the CCM was 8 °C with a cooling differential of 5 K for the internal hysteresis control. A 1<sup>st</sup> order system with delay element behaviour similar to the CHP and the AdCM case is noticed. However, the delay element is much smaller in this case. Within 1 minute of starting the CCM the return-line temperature from the CCM to the CTES drops by 5 K and the machine is in steady state. This 5 K temperature difference is achieved

by the CCM for its given cooling capacity ( $P_{th\_CCM}$ ) and constant volume flow. Thus the stratifications in the CTES occur in 5 K stages.

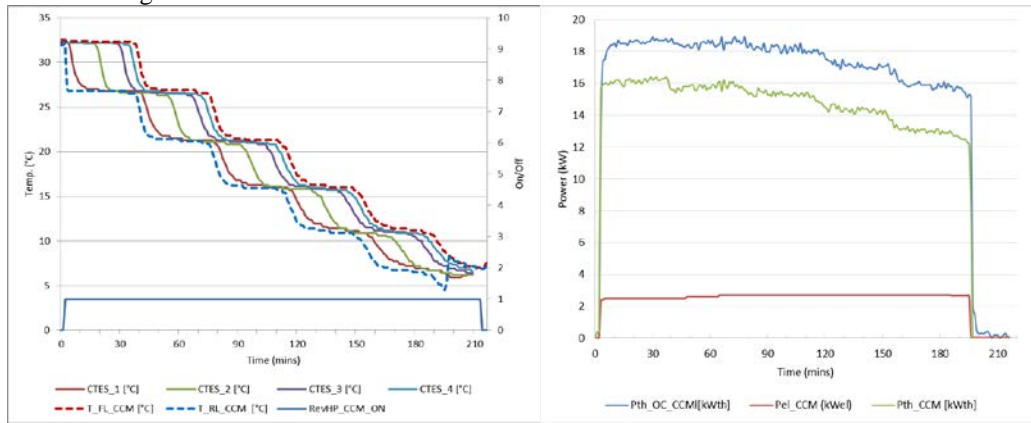


Figure 7 (a & b). Charging of the CTES with CCM

Another expected effect noticed in the fig. 7a is the shutting down of the CCM after operating for 3.25 hours since it achieved the set-point temperature of 8 °C in its feed-line coming from the CTES ( $T_{FL\_CCM}$ ). After it shuts-down internally, the external pumps in the circuit keep running and have a negative effect of mixing the stratifications as seen between 200 and 210 mins of operation. The machine will turn on again when the cooling differential of 5 K is achieved in the  $T_{FL\_CCM}$  i.e. it to  $8 + 5 = 13$  °C. While modelling this system the internal hysteresis control should also be considered so that during optimal control this behaviour could be avoided. A constant volume flow of 2.45 m<sup>3</sup>/h (evaporator) and 2.65 m<sup>3</sup>/h (condenser) is achieved during CCM operation.

Analogous to the relationship of the thermal powers in the AdCM circuit the relationship between the thermal and electrical powers for the CCM can be seen in the fig 7 (b). Here the approximate sum of the cooling capacity of the CCM ( $P_{th\_CCM}$ ) and its electrical input ( $P_{el\_CCM}$ ) is the energy released to the environment over the OC circuit ( $P_{th\_OC\_CCM}$ ). This behaviour is in accordance with the thermodynamic cycle of a heat pump.

### 6.5 Reversible Heat Pump (RevHP) as Heat Pump Heating Performance

Steady state behaviour of the HP is shown in the results of a test in fig.8 (a & b) below. Here the initial temperature of the HTES is 30 °C and no heating loads were connected to the tank. The set temperature for the internal hysteresis of the CCM was 45 °C with a heating differential of 3 k for the internal hysteresis control. A 1st order system with a small delay element behaviour similar to the CHP and the CCM case is noticed. The reason for the stratifications in stages and a constant volume flow is explained in sections 3.3 and 6.4 already.

Also as explained earlier the machine automatically shuts-off after the water returning from the HTES and entering the condenser ( $T_{RL\_HP}$ ) reaches the set point of 45 °C and the machines fluctuates with the heating differential of the 3 K set in the internal control. No significant increase in tank temperatures is noticed and to avoid damage to the machine such frequent switching must be avoided by involving a constraint in the supervisory controller or by controlling the machine over a relevant temperature sensor in the HTES and not  $T_{RL\_HP}$ . A constant volume flow of 2.45 m<sup>3</sup>/h (evaporator) and 2.79 m<sup>3</sup>/h (condenser) is achieved during HP operation. Analogous to AdCM and CCM in fig. 8b it is seen that the heating capacity ( $P_{th\_HP\_HT}$ ) is the approximate sum of the electric power input ( $P_{el\_HP}$ ) and the power in the outdoor coil circuit ( $P_{th\_OC\_HP}$ ).

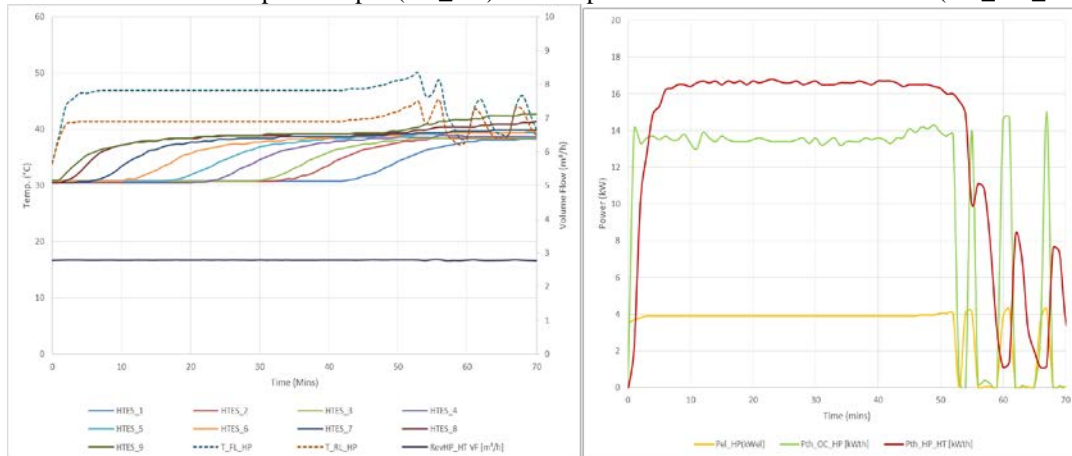


Figure 8 (a & b). Charging of HTES with RevHP

## 7 CONCLUSIONS

The experimental set-up at INES for microscale trigeneration system was explained in detail and results of the functional tests and measurements were described. With the aid of these measurements, important control parameters like safety shut-down temperature of cogeneration units were identified and the importance of including them in the optimal control problem structure was noted. These could be included in the optimal control either as constraints or in the models of the components to ensure control actions closest to the real operational range of the components. Engineering tips for ex. even a simple construction in the hot tank for feeding the hot water from the microscale cogeneration unit works to create a good stratification profile amongst other valuable lessons-learnt were shared.

## 8 ACKNOWLEDGEMENTS

The authors would like to thank the support of the DENE Graduate School in Freiburg and the Reiner Lemoine Stiftung in Berlin.

## REFERENCES

- [1] IEA EBC,(2016),“IEA/ECBCS Annex 54: Integration of Micro-Generation and Related Energy Technologies in Buildings” [Internet]2016. Available from: <http://www.iea-ebc.org/projects/completed-projects/ebc-annex-54/>
- [2] Wu DW, Wang RZ,(2006),“Combined cooling, heating and power: A review”*Prog Energy Combust Sci* [Internet]. 32(5–6):459–95. Available from: <http://www.sciencedirect.com/science/article/pii/S0360128506000244>
- [3] Cho H, Smith AD, Mago P,(2014),“Combined cooling, heating and power: A review of performance improvement and optimization”*Appl Energy* [Internet]. [cited 2015 Jan 27];136:168–85. Available from: <http://www.sciencedirect.com/science/article/pii/S0306261914009301>
- [4] Jradi M, Riffat S,(2014),“Tri-generation systems: Energy policies, prime movers, cooling technologies, configurations and operation strategies”*Renew Sustain Energy Rev* [Internet]. 32:396–415. Available from: <http://dx.doi.org/10.1016/j.rser.2014.01.039>
- [5] Zhao Y, Lu Y, Yan C, Wang S,(2015),“MPC-based optimal scheduling of grid-connected low energy buildings with thermal energy storages”*Energy Build* [Internet]. 86:415–26. Available from: <http://linkinghub.elsevier.com/retrieve/pii/S0378778814008640>
- [6] Ma Y, Borrelli F, Hancey B, Packard A, Bortoff S,(2009),“Model Predictive Control of thermal energy storage in building cooling systems”In: *Proceedings of the 48th IEEE Conference on Decision and Control (CDC) held jointly with 2009 28th Chinese Control Conference* [Internet]. 2009. p. 392–7. Available from: <http://ieeexplore.ieee.org/lpdocs/epic03/wrapper.htm?arnumber=5400677>
- [7] Facci AL, Andreassi L, Ubertini S,(2014),“Optimization of CHCP (combined heat power and cooling) systems operation strategy using dynamic programming”*Energy*. 66:387–400.
- [8] Angrisani G, Akisawa A, Marrasso E, Roselli C, Sasso M,(2016),“Performance assessment of cogeneration and trigeneration systems for small scale applications”*Energy Convers Manag* [Internet]. 125:194–208. Available from: <http://dx.doi.org/10.1016/j.enconman.2016.03.092>
- [9] Becker M, Boris A (HS K, Korbinian S (HS K, Tejaskumar P (HS K, Jost B (HS K,(2013),“Regenerativ betriebene, innovative Kraft-Wärme-Kälte-Kopplungsanlage(InnoKKK)”In: Mayer W, Becker M, Goschy H, editors. *FORETA Ergebnisse des Forschungsverbundes „Energieeffiziente Technologien und Anwendungen“* [Internet]. Munich: Verlag Attenkofer, Straubing; 2013. p. G1–26. Available from: <http://www.hochschule-kempten.de/forschung/allgemeine-projekte/energiesystemtechnik/innokkk-2009-2012/projektbeschreibung.html>
- [10] Henning H-M,(2010),“PolySMART ® POLYgeneration with advanced Small and Medium scale thermally driven Air-conditioning and Refrigeration Technology”Freiburg; 2010.
- [11] Kong XQ, Wang RZ, Wu JY, Huang XH, Huangfu Y, Wu DW, et al.,(2005),“Experimental investigation of a micro-combined cooling, heating and power system driven by a gas engine”*Int J Refrig*. 28(7):977–87.
- [12] Bruni G, Cordiner S, Mulone V, Rocco V, Spagnolo F,(2015),“A study on the energy management in domestic micro-grids based on Model Predictive Control strategies”*Energy Convers Manag* [Internet]. [cited 2016 Feb 23];102:50–8. Available from: <http://www.sciencedirect.com/science/article/pii/S0196890415000801>

- 
- [13] Angrisani G, Rosato A, Roselli C, Sasso M, Sibilio S,(2012),“Experimental results of a micro-trigeneration installation”*Appl Therm Eng* [Internet]. [cited 2015 Oct 23];38:78–90. Available from: <http://www.sciencedirect.com/science/article/pii/S1359431112000208>
- [14] Dagdougui H, Minciardi R, Ouammi A, Robba M, Sacile R,(2012),“Modeling and optimization of a hybrid system for the energy supply of a ‘Green’ building”*Energy Convers Manag* [Internet]. 64:351–63. Available from: <http://www.sciencedirect.com/science/article/pii/S0196890412002373>
- [15] Sawant P, Pfafferott J,(2015),“Experimental Analysis of Microscale Trigeneration Systems to Achieve Thermal Comfort in Smart Buildings”In: *The Proceedings of the 36th AIVC Conference*. Madrid; 2015.
- [16] SenerTech GmbH,(2014),“Planungshandbuch Dachs Gen1.1” [Internet]2014 [cited 2017 May 4]. p. 108. Available from: <http://senertec-center.com/wordpress/index.php/daten-fakten/>
- [17] Aral Forschung,(2016),“Aral HeizölEcoPlus” [Internet]2016 [cited 2016 Sep 29]. Available from: <http://www.aral-heizoel.de/partner/prescher/heizoel/aran-heizoel/aran-heizoel-eco-plus.html>
- [18] SorTech AG,(2014),“SorTech eCoo Operating Manual” [Internet]2014 [cited 2017 Mar 29]. Available from: <http://www.sortech.de/en/products/our-products/>
- [19] Daikin Europe,(2016),“Daikin HydroCube” [Internet]2016 [cited 2016 Sep 12]. Available from: [http://www.daikin.de/docs/ECPEN15-462\\_1\\_LR-tcm478-377595.pdf](http://www.daikin.de/docs/ECPEN15-462_1_LR-tcm478-377595.pdf)
- [20] HT HelioTech GmbH,(2017),“Operating Strategies Stratified Tank” [Internet]2017 [cited 2017 Mar 29]. Available from: [www.ht-heliotech.de](http://www.ht-heliotech.de)
- [21] Eicker U,(2006),“Storage Modelling”In: *Solar Technologies for Buildings*. Stuttgart: John Wiley & Sons; 2006. p. 97–103.
- [22] De Césaró Oliveski R, Krenzinger A, Vielmo H a.,(2003),“Comparison between models for the simulation of hot water storage tanks”*Sol Energy*. 75(2):121–34.
- [23] Streckiene G, Martinaitis V, Vaitiekunas P,(2011),“Simulation of Thermal Stratification in the Heat Storage for CHP Plant”In: *The 8th International Conference Environmental Engineering*. Vilnius; 2011. p. 812–9.
- [24] Tuerk + Hillinger GmbH,(2016),“Immersion Heater Type EHK” [Internet]2016 [cited 2016 Sep 10]. Available from: <http://www.tuerk-hillinger.de/en-US/products/products/ehk-immersion-heater/>,
- [25] Labs I,(2016),“PT 100 Resistance Table” [Internet]2016 [cited 2016 Oct 7]. Available from: [http://www.ietlabs.com/pdf/Datasheets/Pt100Temperature\\_Resistance4digits.pdf](http://www.ietlabs.com/pdf/Datasheets/Pt100Temperature_Resistance4digits.pdf)
- [26] Bracco S, Delfino F, Pampararo F, Robba M, Rossi M,(2014),“A mathematical model for the optimal operation of the University of Genoa Smart Polygeneration Microgrid: Evaluation of technical, economic and environmental performance indicators”*Energy* [Internet]. [cited 2015 May 27];64:912–22. Available from: <http://www.sciencedirect.com/science/article/pii/S0360544213008918>
- [27] Seifert J,(2013),“Mikro BHKW Systeme Für Den Gebäude Bereich”Berlin: VDE Verlag GmbH; 2013.
- [28] Núñez T,(2010),“Thermally Driven Cooling: Technologies, Developments and Applications”*J Sustain Energy* [Internet]. 1(4):16–24. Available from: [http://www.energy-cie.ro/archives/2010/nr\\_4/v4-03\\_nunez\\_thomas.pdf](http://www.energy-cie.ro/archives/2010/nr_4/v4-03_nunez_thomas.pdf)
- [29] Schicktanz M, Núñez T,(2009),“Modelling of an adsorption chiller for dynamic system simulation”*Int J Refrig*. 32(4):588–95.
- [30] Gräber M, Kirches C, Bock HG, Schlöder JP, Tegethoff W, Köhler J,(2011),“Determining the optimum cyclic operation of adsorption chillers by a direct method for periodic optimal control”*Int J Refrig* [Internet]. [cited 2017 May 21];34(4):902–13. Available from: <http://www.sciencedirect.com/science/article/pii/S0140700710002963>